The *s-d* exchange model as the underlying mechanism of magnetoresistance in ZnO doped with alkali metals

C Zapata[1], G Nieva[2], J M Ferreyra[1], M Villafuerte[1], L Lanoël[2], G Bridoux[1]

[1] Laboratorio de Física del Sólido, INFINOA (CONICET-UNT), Facultad de Ciencias Exactas y Tecnología, Universidad Nacional de Tucumán, 4000 San Miguel de Tucumán, Argentina

[2] Centro Atómico Bariloche-CNEA, Instituto Balseiro-Universidad Nacional de Cuyo and CONICET, 8400 S. C. Bariloche, Argentina

E-mail: gbridoux@herrera.unt.edu.ar

August 2017

Abstract. High field magnetoresistance has been studied in epitaxial n-type ZnO:Na and ZnO:Li thin films in a temperature range between 4 K and 150 K. The resulting negative magnetoresistance can be well fitted using a semiempirical model of Khosla and Fischer based on third order contributions to the *s-d* exchange Hamiltonian. The parameters obtained from this model were carefully analyzed. One of these parameters is related to a ratio between electron mobilities at zero field (a non-exchange scattering mobility μ_0 and an exchange or spin dependent one μ_J). From Hall effect measurements μ_0 was obtained, displaying a weak temperature dependence in accordance with highly n-doped ZnO while the extracted μ_J exhibits an anomalous T-dependence. On the other hand, our magnetoresistance data cannot be properly fitted using Kawabata's expression based on a weak-localization model.

1. Introduction

When a few atomic percent of Manganese is replaced by Galium in GaAs, this semiconductor becomes ferromagnetic below a Curie temperature $T_C \sim 110$ K [1]. This was a remarkable discovery that allowed the development of spintronic in semiconductors in the following years [2]. Despite there is still a debate about the origin of ferromagnetism in this III-V semiconductor, there is one model that stands among the rest: The *p-d* or *s-d* exchange model. In this picture, the itinerant carriers (which are presumably holes donated by Mn in the case of $Ga_{1-x}Mn_xAs$) experiment an exchange interaction with the localized magnetic moments (the Mn ones in $Ga_{1-x}Mn_xAs$) giving rise to a magnetic order. The effect observed in $Ga_{1-x}Mn_xAs$ triggered the research in others potential dilute magnetic semiconductors (DMS) like ZnO or GaN where room temperature ferromagnetism was predicted when they are p-doped [3, 4, 5]. This latter

issue becomes a materials science challenge in the II-VI semiconducting ZnO since it naturally becomes n-type and the stability of acceptors in this material is rather low [6, 7]. Moreover, the doping with magnetic elements like Mn should be carefully performed [8, 9] since impurity clusters, spurious magnetic phases or an inhomogeneous distribution of magnetic impurities in the sample can generate magnetic signals which are the responsible of the wide variety of T_C values found in ZnO ranging from 0 to 1000 K [10, 11].

Alternatively, it has been predicted that acceptor doping with non-magnetic elements like Li or Na stabilizes the formation of Zinc vacancies V_{Zn} [6, 12, 13, 14]. Moreover, recent works have proposed and also shown evidence of V_{Zn} as localized magnetic defects in ZnO [15, 16]. Doping of ZnO with Na or Li has been previously performed in a wide variety of micro and nano-structures in search of the development of optical and optoelectronic devices [6, 12, 13, 14, 17, 18, 19, 20, 21, 22]. It has been found that the optimal Li or Na doping that generates substitutional defects like Zn_{Li} or Zn_{Na} (which are the ones that stabilize the V_{Zn}) without producing a significant amount of interstitial ones (which are donors) is around 5 at.% [13, 14]. Above this concentration, interstitial doping starts to increase compensating the acceptor ones.

One of the key effects when itinerant electrons interact with localized magnetic moments is the presence of negative magnetoresistance (MR) [23, 24, 25], a relevant property for spintronic applications [2] and a more subtle technique to analyze the DMS. In the case of ZnO, this effect has been observed in n-doped samples [26, 27, 28, 29] with MR values between 3 and 7 % at $T \sim 5 - 10$ K. For electron carrier concentrations lower than $n \sim 3 \times 10^{18}$ cm^{-3}, the negative magnetoresistance is overpassed by an enhanced positive magnetoresistance [26, 28] in accordance to a two-band model (an impurity plus a conduction band) [30, 31]. The negative MR in ZnO can be well described using a phenomenological model originally proposed by Khosla and Fischer to account for their experiments in n-type CdS [31]. In their model, Khosla and Fischer adapt expressions for negative MR previously developed by Appelbaum based on third order terms of the *s-d* Hamiltonian [32] in the context of a tunneling problem between two metals with magnetic impurities at the interface. This adaptation requires an appropriate transformation of tunneling rates to scattering rates [31] in order to provide an adequate interpretation of the parameters involved in the model. In this work, we provide a detailed study of the physics behind these parameters in MR measurements on n-type ZnO films doped with non-magnetic elements (Na and Li).

2. Experimental Details

Starting from ZnO powders doped with 5 at.% of Na or Li synthesized as described in Ref. [14], corresponding ceramic targets were fabricated. Then, high quality oxygen deficient ZnO:Na and ZnO:Li thin films were grown on sapphire (0001) substrates (dimensions: $(5 \times 5 \times 0.5)$ mm^3) by pulsed laser deposition (PLD) at a temperature of 550°C and an oxygen pressure between 0.05 and 0.5 mTorr using a Nd:YAG laser

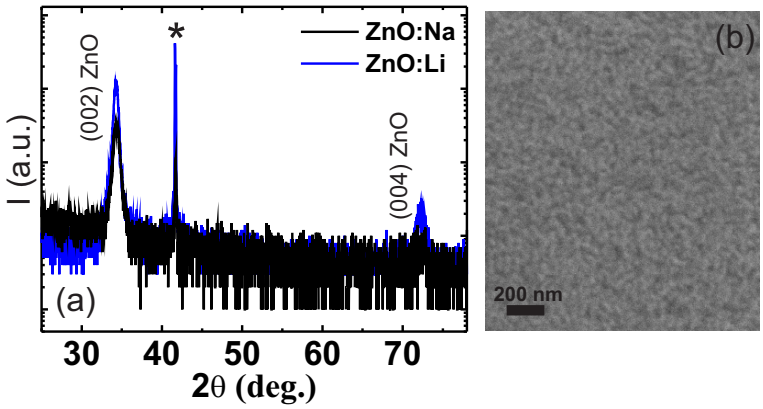

Figure 1. (a) $\theta - 2\theta$ scans of ZnO:Na (black line) and ZnO:Li (blue line) films grown on (0001) sapphire. The (002) and (004) ZnO peaks are present for both type of films. The peak corresponding to a reflection of the sapphire substrate is labeled with an asterisk. (b) SEM image of the ZnO:Na film surface.

operated with a wavelength of 266 nm, a repetition rate of 10 Hz and an energy density of 2.1 J/cm^2 [33]. The deposition rate was $\sim$ 0.018 nm s^{-1} and the film thicknesses are of $\simeq$ 54 nm. EDX mapping studies show an homogenous incorporation of Na in the ZnO:Na films while in the case of ZnO:Li films the Lithium was not able to be observed probably due to its low atomic weight. X-ray diffraction measurements were performed in the films using CuKα radiation (λ = 0.15406 nm), see $\theta - 2\theta$ scans in Fig. 1a. The resulting films have epitaxially grown along the c-axis direction with a wurtzite structure and without any spurious phase, see Fig. 1a. For both films, the position of the (002) peak is shifted to lower angles ($2\theta \simeq 34.28°$ and 34.31° for the ZnO:Na and ZnO:Li films respectively) compared to bulk ZnO ($2\theta \simeq 34.42°$) [34]. From the position of these peaks, the corresponding c lattice parameter can be determined using the expression $1/d^2_{hkl} = l^2/c^2 + 4(h^2 + k^2 + h.k)/3a^2$, where (h, k, l) are the Miller indices. Resulting values of c = 5.227 Å and c = 5.223 Å are obtained for the ZnO:Na and ZnO:Li films respectively. These values are higher than the bulk ZnO c-lattice parameter (c = 5.207 Å) indicating that both films are slightly tensile strained (around 0.3%) in the c-axis direction. In order to quantify the grain size of our films we have extracted the full width at half maximum (FWHM) of the corresponding (002) peaks for both films (giving $w = 0.72°$ and 0.52° for the ZnO:Na and ZnO:Li films respectively) and we have made use of the Scherrer equation $\langle D \rangle = K\lambda/(w\, cos\theta)$ with $K \sim 0.94$ [35]. The resulting grain size values are similar for both films being $\langle D_{Na} \rangle \simeq 12$ nm and $\langle D_{Li} \rangle \simeq 17$ nm for the ZnO:Na and ZnO:Li respectively. In Fig. 1b, a SEM image of the ZnO:Na film surface shows small grains with similar sizes to the ones estimated above.

Magnetoresistance measurements were carried out in a cryostat equipped with a rotating sample holder at temperatures between 4 and 150 K and magnetic fields up to 16 T. We have employed the four-point-probe method using Indium ohmic contacts and a configuration with the applied magnetic field H parallel to the electrical current

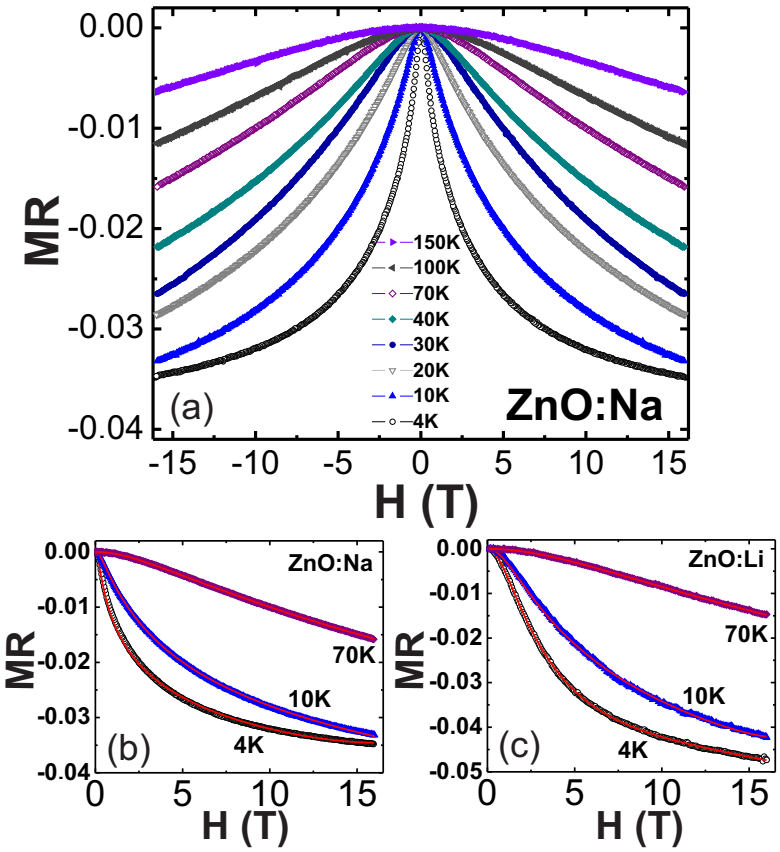

Figure 2. (a) Magnetic field dependence of MR at different temperatures for the ZnO:Na film. As it can be noticed, the MR signal increases as the temperature is reduced. A Comparison between the MR data and the corresponding fittings (red lines) using Eq. (1) is presented for ZnO:Na (b) and ZnO:Li films (c).

density I, $I \parallel H$. High electron carrier densities ($n \simeq 10^{20}\,\mathrm{cm}^{-3}$) have been obtained in our films by Hall effect measurements using the Van der Pauw method. No evidence of anomalous Hall effect has been observed [36]. Magnetization measurements have been performed using a SQUID at temperatures ranging from 4 to 300 K and applied magnetic fields up to 5 T. Remarkably, our films do not present a magnetic signal within the experimental error ($\sim 10^{-6}$ emu). For $\sim 10^{-6}$ emu, a simple estimation gives a total amount of $\sim 5 \times 10^{13}$ localized magnetic moments. This value corresponds to a few at.% of these moments in our sample.

3. Results and Discussion

The field dependence of MR (defined as $(\rho - \rho(H = 0))/\rho(H = 0)$) at different temperatures is presented in Fig. 2 for ZnO:Na and ZnO:Li films. As it can be observed, the negative MR signal increases as the temperature is decreased. The negative MR value at $T = 4\,\mathrm{K}$ and $H = 16\,\mathrm{T}$ reaches $\sim 3.4\%$ and $\sim 4.7\%$ for ZnO:Na and ZnO:Li

respectively in agreement with the values reported for ZnO doped with non magnetic elements and carrier densities above $\sim 3 \times 10^{18}\,\mathrm{cm}^{-3}$ [26, 28, 29].

MR expressions based on second order terms of the $s-d$ Hamiltonian [23, 24, 25] lead to a $MR \propto -H^2$ dependence which can not properly fit our MR data. In order to evaluate the negative MR taking into account third order terms of the s-d Hamiltonian, Appelbaum [32] developed a model based on the transmittance of electrons across a tunneling barrier with local magnetic impurities at the interface. In the context of this problem, the exchange and non-exchange interaction with these impurities improves the tunneling of electrons between the two metals. The adaptation of this model to bulk semiconductors where dilute local magnetic moments are present is not straightforward and it requires an adequate transformation of the tunneling probabilities due to an interaction with magnetic (T_J^2) and non-magnetic impurities (T_0^2) to corresponding cross-sections or scattering rates. As it was already noticed, the first adaptation was proposed by Khosla and Fischer [31] to account for their negative MR data on CdS semiconducting single crystals doped with In. After several approximations they found that MR can be expressed as:

$$MR = -a^2 \ln(1 + b^2 H^2) + \frac{c^2 H^2}{1 + d^2 H^2} \tag{1}$$

where the last term corresponds to a well known positive MR contribution deduced from a two band model [30, 31]. The parameters c and d are related to the conductivities and mobilities of these two bands [37]. On the other hand, the parameters a and b that appear in the negative MR contribution are defined as [31]:

$$a^2 = a_1^2[S(S+1) + \langle M^2 \rangle] \tag{2}$$

$$b^2 = \left[1 + 4S^2\pi^2 \left(\frac{2J\rho_F}{\mathrm{g}}\right)^4\right] \frac{\mathrm{g}^2\mu_B^2}{(\alpha k_B T)^2} \tag{3}$$

where g is the Landé factor, μ_B is the Bohr magneton, S is the spin of the localized moment, J is the exchange integral resulting from the interaction between the itinerant electron and the localized magnetic moment and ρ_F is the density of states at the Fermi energy level. α is a numerical factor close to $\alpha \simeq 1$ introduced by Appelbaum [32, 38, 39]. As it can be noticed, the term $(bH)^2$ is proportional to $(\mathrm{g}\mu_B H/k_B T)^2$, hence the electronic conduction will be improved as the magnetic energy of the local moments grows in relation to the thermal energy, see Eq. (1). The term a_1^2 can be expressed as $a_1^2 = 2J\rho_F A_1$, where A_1 is related to a ratio between the cross-section due to exchange scattering with magnetic impurities, σ_J, and the cross-section due to other non-exchange scattering mechanisms, σ_0, (non-magnetic impurities, phonons). Appelbaum [32] proposed that $\langle M^2 \rangle$ is expressed by:

$$\langle M^2 \rangle = \langle M \rangle^2 - (S + \frac{1}{2})^2 \sinh^{-2}(S + \frac{1}{2}) \frac{\mathrm{g}\mu_B H}{k_B T} + \frac{1}{4} \sinh^{-2} \frac{\mathrm{g}\mu_B H}{2k_B T} \tag{4}$$

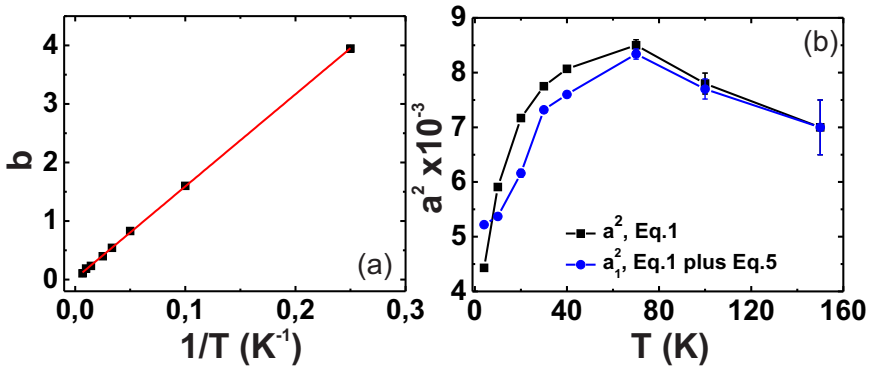

Figure 3. Parameters obtained by fitting the ZnO:Na MR data with Eq. (1). (a) $1/T$-dependence of parameter b. A linear fit (red line) using Eq. (3) is also shown. (b) Temperature dependence of the parameter a^2 (black squares). If Eq. (2) and Eq. (5) are explicitly included in the fittings of the MR data with Eq. (1), a resulting T-dependent a_1^2 is obtained (blue circles).

where $\langle M \rangle$ is the normalized magnetization and the last two terms constitute a magnetization variance. Using the Brillouin function for $\langle M \rangle$ and reordering terms through hyperbolic functions identities Eq. (4) can be expressed in the case S=1/2 as:

$$\langle M^2 \rangle = \frac{1}{4} + \frac{3}{4} \tanh^2 \frac{g\mu_B H}{2k_B T} \tag{5}$$

Hence the ratio $(g\mu_B H/k_B T)$ intervenes in $\langle M^2 \rangle$ as well as in the term $(bH)^2$. At first sight, it can be noticed that $\langle M^2 \rangle$ has a weak T-dependence in the range of temperatures explored. The resulting fittings using Eq. (1) are in excellent agreement with our data, see Fig. 2b and Fig. 2c. In what follows our analysis will be focused on the ZnO:Na data even though similar results have been obtained for ZnO:Li.

The temperature dependence obtained for the parameter b is in good agreement with the predicted by Eq. (3), as it can be observed in Fig. 3a. Taking g=2 and S=1/2, which are values corresponding to a local moment formed by a Zinc vacancy, V_{Zn}, [15] it is possible to extract $J\rho_F$ from Eq. (3) using the fitting values obtained in Fig. 3a. It gives a value of $J\rho_F = 1.9$ in accordance with the ones reported in ZnO which range between $\sim$ 1.7 and $\sim$ 2.1 [26, 29]. As it can be observed in Fig. 3b, the resulting parameter a^2 (see Eq. (1)) has a temperature dependence outside the margins of error. This is an unexpected result considering that previous reports on ZnO suggest that a^2 does not vary with temperature [26, 29]. Since the term $\langle M^2 \rangle$ is T-dependent (see Eq. (5)) and it takes part in a^2 (see Eq. (2)) we have explicitly included this temperature dependence of $\langle M^2 \rangle$ in Eq. (1) and we have performed new fittings with this modified expression to our data. Again, these new fittings are in good agreement with our MR measurements and the resulting parameters remain unchanged compared with the previous ones within the margins of error. In particular, we have compared the a^2 values obtained from the previous fittings with the a_1^2 values resulting from these new fittings, see Fig. 3b. As it can be noticed, the values of a^2 and a_1^2 and their T-dependence are

basically the same within the error. It means that the temperature dependence of $\langle M^2 \rangle$ is not a significant contribution to a^2 (see Eq. (2)) and that it mainly comes from the term a_1^2.

Within the frame of the tunneling problem studied by Appelbaum [32] a_1^2 can be written as $a_1^2 \simeq 2J\rho_F T_J^2/T_0^2$ if $T_0^2 \gg T_J^2$. In the case of bulk semiconductors, Khosla and Fischer [31] express a_1^2 in terms of corresponding cross-sections as $a_1^2 \simeq 2J\rho_F N_J \sigma_J^2/\sigma_0^2$, where N_J is the density of localized magnetic moments. In the following, we are going to show that if MR is simply expressed in terms of corresponding cross-sections using the Drude model and the Matthiessen rule, the resulting a_1^2 differs from the one deduced by Khosla and Fischer [31].

Lets assume that $\sigma(H) = \sigma_0 + \sigma_J(H)$ with $\sigma(H = 0) = \sigma_0 + \sigma_J(H = 0)$ and $\rho = (m^* v_F/ne^2) \sum_i N_i \sigma_i$ where $i = 0$ or J, n is the electron carrier density, m^* is the effective mass of the electron, v_F is the Fermi speed and N_i is the corresponding density of scattering centers. If we define $\sigma_J(H) = \sigma_J(H = 0)F(H)$ where $F(H)$ takes into account the magnetic field dependence, MR can be expressed as:

$$\begin{aligned} &\frac{\rho - \rho(H=0)}{\rho(H=0)} \simeq -\frac{N_J \sigma_J(H=0)}{N_0 \sigma_0}(F(H) - 1) \\ &= -\frac{\mu_0}{\mu_J(H=0)}(F(H) - 1) \end{aligned} \tag{6}$$

where $\mu_i = e/(m^* v_F N_i \sigma_i)$ are the electron mobilities and it was assumed that $\sigma_0 \gg \sigma_J(H = 0)$. If a general comparison between the prefactor of Eq. (6) and the parameter a^2 in the first term of Eq. (1) is made, it is possible to express a^2 approximately as:

$$a^2 \simeq a_1^2 \simeq \frac{2J\rho_F N_J \sigma_J(H=0)}{N_0 \sigma_0} = \frac{2J\rho_F \mu_0}{\mu_J(H=0)} \tag{7}$$

Unlike Khosla and Fischer [31], we find a simple linear relation between a_1^2 and the ratio of corresponding cross-sections, see Eq. (7). In addition, Eq. (7) establishes that a_1^2 represents the ratio between the electronic mobility due to non-exchange scattering mechanisms and the one due to exchange scattering mechanisms (including spin flip and non-spin flip events). The previous assumption $\sigma_0 \gg \sigma_J(H = 0)$ implies that $\mu_0 \ll \mu_J(H = 0)$ hence if the Matthiessen rule is valid, the total electron mobility μ_T will be dominated by μ_0 which would be the major contributor to the measured electron mobility. Consequently, measuring the electron mobility and using the values of a_1^2 extracted from Fig. 3b it is possible to obtain $\mu_J(H = 0)$ via Eq. (7).

In Fig. 4a and Fig. 4b we present the temperature dependence of both the electron carrier concentration obtained from Hall effect measurements and the electrical resistivity respectively. Both of them have a weak temperature dependence in the same way as the resulting electron mobility $\mu_T \simeq \mu_0$, see Fig. 4c. This weak T-dependent mobility at high doping levels in ZnO has been already predicted by Alfaramawi [40].

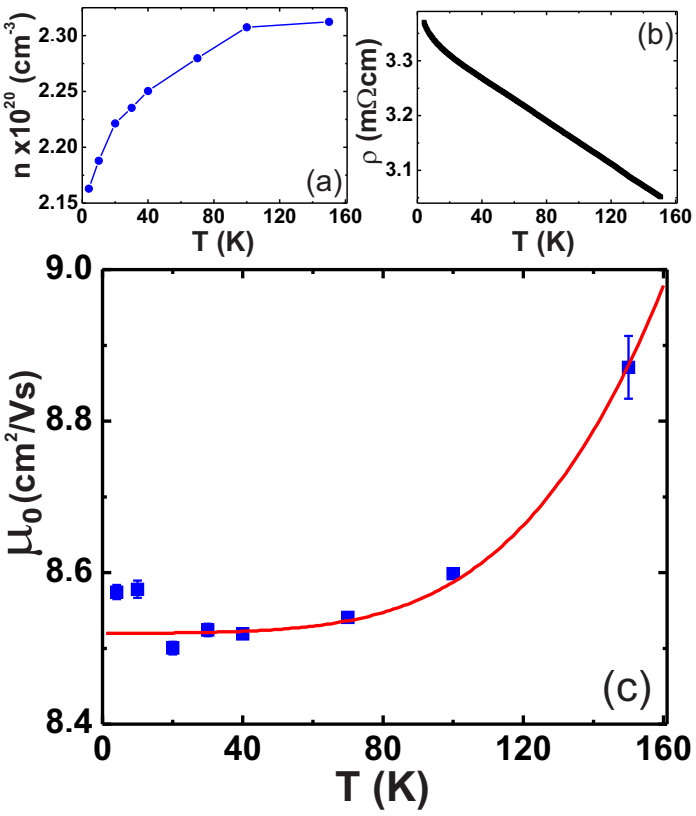

Figure 4. Temperature dependence of both the electron carrier density (a) and the electrical resistivity (b) for the ZnO:Na film. (c) Resulting Hall electron mobility, μ_0, (blue squares) as a function of the temperature. A corresponding fitting using Alfaramawi's expression [40] (red curve) is also shown.

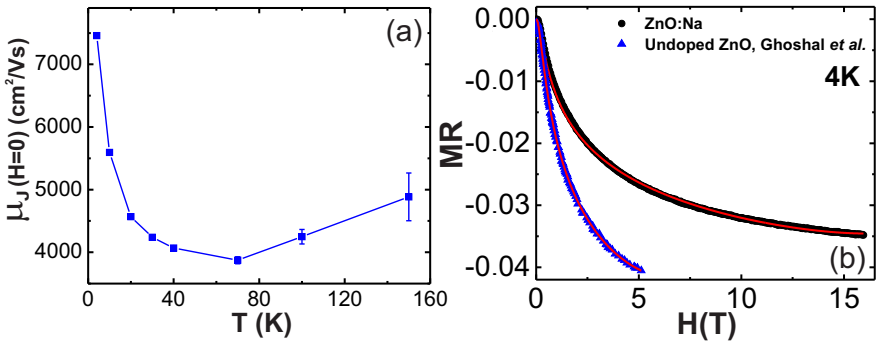

Figure 5. (a) Extracted zero field electron mobility due to exchange (or spin) dependent scattering mechanisms for the ZnO:Na film. $\mu_J(H=0)$ starts to increase as the temperature is decreased below $T \simeq 70\,\mathrm{K}$. (b) Field dependent MR at $T \simeq 4\,\mathrm{K}$ for the ZnO:Na film (black circles) and for an undoped ZnO film (blue triangles) adapted from Ghoshal *et al.* Ref. [28]. Red lines are the corresponding fittings using Eq. (1).

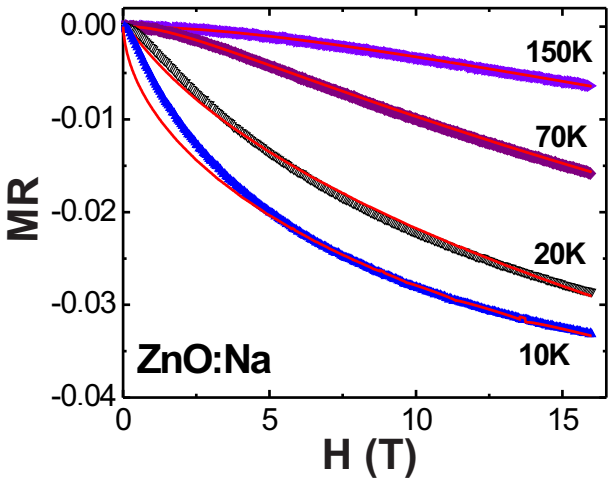

Figure 6. Field dependent magnetoresistance at different temperatures for the ZnO:Na film. The red curves are corresponding fittings using Eq. (8). The obtained phase-coherence length values are ℓ_φ= 500 nm ($T = 10$ K), 43 nm ($T = 20$ K), 13.3 nm ($T = 70$ K) and 6.85 nm ($T = 150$ K).

In his model, scattering with ionized impurities and phonons are included as well as the electron-electron interaction [40, 41, 42]. Using the parameters adopted by Alfaramawi [40] in ZnO with an ionized impurity concentration of $1 \times 10^{20}\,\mathrm{cm}^{-3}$, a good agreement between this model and our experimental values is obtained, see Fig. 4c.

As it was pointed out, knowing the values of μ_0 and a_1^2 it is possible to extract $\mu_J(H = 0)$ using Eq. (7), the results are showed in Fig. 5a. As it can be observed, $\mu_J(H = 0)$ is weakly T-dependent at $T > 70$ K which seems to be consistent with the behavior predicted by second order terms of the s-d exchange model [23, 25]. A departure from this behavior is observed at $T < 70$ K, that is to say, $\mu_J(H = 0)$ increases as temperature is decreased, see Fig. 5a. This enhancement of the exchange (or spin) mobility at low-T does not seem to be caused by an increase of the localized magnetic moments order since this has already been taken into account in the term $(bH)^2$ and $\langle M^2 \rangle$, see Eq. (1) and Eq. (2). Further studies are needed to provide a deeper understanding of this effect.

It is worth to compare the MR of our ZnO films doped with alkali metals with the one corresponding to undoped ZnO films which is well established in the literature [26, 27, 28, 43]. In Fig. 5b the MR of our ZnO:Na film and the one for an undoped ZnO film [28] are compared. The resulting fittings using Eq. (1) lead to a value of $J\rho_F \simeq 1.9$ for the undoped ZnO film which is equal to the value obtained for our ZnO:Na film. This result suggests that the localized magnetic defect that is responsible for the exchange mechanism with the itinerant electrons is the same for both films, pointing to an intrinsic defect (i.e. Zinc vacancies). In the case of the undoped ZnO film, the parameter $a^2_{undoped} = 0.00734$ at $T \simeq 4$ K is higher than the one obtained

for the ZnO:Na film at the same temperature ($a^2_{Na} = 0.00443$, see Fig. 3b); the ratio between these two values being ~ 1.7. Using Eq. (7) for each film and assuming that $\mu_0^{Na} \simeq \mu_0^{undoped}$ one obtains that $\mu_J^{Na} \simeq 1.7\mu_J^{undoped}$.

On the other hand, it is worth to ask if our ZnO films are outside the strong localization regime [44, 45]. A simple estimation using the quantities showed in Fig. 4 allows us to estimate $k_F l$ for our films, where k_F is the Fermi wave-vector and l is the mean free path. It gives a value of $k_F l \simeq 1.8 > 1$, which means that we are in a regime where the weak scattering theory still works [45] and the Khosla model [31] can be applied. In this regard, Ajimsha *et al.* [46] have considered that their MR data in Ga-doped ZnO films can be explained in the context of phase coherent electron transport. They have used a weak-localization expression [47] which accounts for the negative magnetoresistance plus a positive contribution arising from the electron-electron interaction [46] to fit their data:

$$MR = \left(\frac{\Delta\rho}{\rho(H=0)}\right)_{WL} + \left(\frac{\Delta\rho}{\rho(H=0)}\right)_{EE} \tag{8}$$

where:

$$\left(\frac{\Delta\rho}{\rho(H=0)}\right)_{WL} = \frac{-e^2\rho(H=0)}{2\pi^2\hbar}\sqrt{\frac{eH}{\hbar}}f_3(\delta) \tag{9}$$

with $\delta = \hbar/(4eH\ell_\varphi^2)$. The phase-coherence length is represented by ℓ_φ. The function $f_3(\delta)$ can be expressed as [47]:

$$f_3(\delta) = \sum_{N=0}^{\infty}[2\left(\sqrt{N+1+\delta} - \sqrt{N+\delta}\right) - \frac{1}{\sqrt{N+1/2+\delta}}] \tag{10}$$

The MR contribution due to electron-electron interaction can be written as [46]:

$$\left(\frac{\Delta\rho}{\rho(H=0)}\right)_{EE} = \frac{e^2\rho(H=0)F_\sigma}{4\pi^2\hbar}\sqrt{\frac{k_BT}{2D\hbar}}g_3(h) \tag{11}$$

where $D = \mu_0 k_B T/e$ is the electron diffusion constant, F_σ is the Coulomb interaction parameter and $h = \mathrm{g}\mu_B H/k_B T$. The function $g_3(h)$ is expressed by:

$$g_3(h) = \int_0^\infty d\Omega \frac{d^2}{d\Omega^2}(\Omega N(\Omega))[\sqrt{\Omega+h} + \sqrt{|\Omega-h|} - 2\sqrt{\Omega}] \tag{12}$$

where $N = 1/(e^\Omega - 1)$. We have tried to fit our MR data with Eq. (8) taking ℓ_φ and F_σ as fitting parameters. The best fit to our data was achieved fixing F_σ at a value of $\simeq 0.3$ for all T. The electron diffusion constant D was determined at each temperature using the Hall mobility values from Fig. 4c. The resulting fittings are shown in Fig. 6. As it can be observed, a good agreement is only attained at high temperatures, while at low temperatures it is not possible to obtain a proper fit to our MR data using Eq. (8), especially at low magnetic fields. This disagreement with the weak-localization model at low-T and low-H has already been observed by Andrearczyk *et al.* [43] in ZnO films.

4. Conclusions

In conclusion, we have successfully applied the Khosla model based on the *s-d* exchange Hamiltonian to our negative MR data on oxygen deficient ZnO:Na and ZnO:Li films. The incorporation of these dopants does not seem to affect the MR signal suggesting that intrinsic defects (i.e. Zinc vacancies) play the role of the localized magnetic defects. We have found an anomalous temperature dependence in one of the model's parameter, a^2. After a careful analysis we have concluded that this temperature dependence comes from a ratio between a non-exchange and a zero field exchange electron mobility, $\mu_0/\mu_J(H=0)$. While the high n-doping level of our films (mainly originated by oxygen vacancies) leads to a weak T-dependent non-exchange mobility, the resulting zero field exchange (or spin) mobility increases when temperature is lowered below $T \sim 70\,\mathrm{K}$.

Acknowledgments

This work was supported by PICT- No. 2016-3356, SCAIT- No. E653, PIP- No. 585, SNMAG and SINALA facilities. We acknowledge the technical assistance of B. Straube and V. F. Correa.

References

[1] Ohno H 1998 Science **281** 951
[2] Dietl T, Awschalom D D, Kaminska M and Ohnno H. 2008 *Spintronics, Semiconductors and Semimetals Series* **82** (Amsterdam: Academic Press/Elsevier)
[3] Dietl T, Ohno H, Matsukura F, Cibert J and Ferrand D 2000 Science **287** 1019
[4] Sato K, Bergqvist L, Kudrnovský J, Dederichs P H, Eriksson O, Turek I, Sanyal B, Bouzerar G, Katayama-Yoshida H, Dinh V A, Fukushima T, Kizaki H and Zeller R 2010 Rev. Mod. Phys. **82** 1633
[5] Dietl T 2010 Nat. Mater. **9** 965
[6] Park C H, Zhang S B and Wei S -H 2002 Phys. Rev. B **66** 73202
[7] Norton D P, Heo Y W, Ivill M P, Ip K, Pearton M F, Chisholm S J and Steiner T 2004 J. Materials Today **7** 34
[8] Sharma P, Gupta A, Rao K V, Owens F J, Sharma R, Ahuja R, Osorio Guillen J M, Johansson B and Gehring G A 2003 Nat. Mater. **2** 673
[9] Jin Z, Hasegawa K, Fukumura T, Zoo Y Z, Hasegawa T, Koinuma H and Kawasaki M 2001 Physica E **10** 256
[10] Di Marco I, Thunstrom P, Katsnelson M I, Sadowski J, Karlsson K, Lebegue S, Kanski J and Eriksson O 2013 Nat. Comm. **4** 2645
[11] Bergqvist L, Eriksson O, Kudrnovsky J, Drchal V, Korzhavyi P and Turek I 2004 Phys. Rev. Lett. **93** 137202
[12] Yi J B, Lim C C, Xing G Z, Fan H M, Van L H, Huang S L, Yang K S, Huang X L, Qin X B, Wang B Y, Wu T, Wang L, Zhang H T, Gao X Y, Liu T, Wee A T S, Feng Y P and Ding J 2010 Phys. Rev. Lett. **104** 137201
[13] Ferreyra J M, Bridoux G, Villafuerte M, Straube B, Zamora J, Figueroa C A and Heluani S P 2017 Sol. Stat. Comm. **257** 42
[14] Straube B, Bridoux G, Zapata C, Ferreyra J M, Villafuerte M, Simonelli G, Esquinazi P, Rodríguez Torres C and Heluani S P 2018 Phys. Stat. Solidi B **255** 1800056

[15] McCluskey M D and Jokela S J 2009 J. Appl. Phys. **106** 071101
[16] Lorite I, Straube B, Ohldag H, Kumar P, Villafuerte M, Esquinazi P, Rodríguez Torres C E, Heluani S P, Antonov V N, Bekenov L V, Ernst A, Hoffmann M, Nayak S K, Adeagbo W A, Fischer G and Hergert W 2015 Appl. Phys. Lett. **106** 082406
[17] Zeng Y J, Ye Z Z, Lu J G, Xu W Z, Zhu L P and Zhao B H 2006 Appl. Phys. Lett. **89** 42106
[18] Lai J J, Lin Y- J, Chen Y- H, Chang H- C, Liu C- J, Zou Y- Y, Shih Y- T and Wang M- C 2011 J. Appl. Phys. **110** 013704
[19] Lv J, Huang K, Chen X, Zhu J, Cao C, Song X and Sun Z 2011 Optics Communications **284** 2905
[20] Swapna R, Santhosh and Kumar M C 2013 Mater Sci. Eng. B-Adv **178** 1032
[21] Polat I 2014 J Mater Sci: Mater Electron **25** 3721
[22] Akcan D, Gungor A and Arda L 2018 J. Molecular Structure **1161** 299
[23] Yosida K 1957 Phys. Rev. **107** 396
[24] Toyozawa Y 1962 J. Phys. Soc. Japan **17** 986
[25] Kondo J 1970 Sol. Stat. Phys. **23** 183
[26] Reuss F, Frank S, Kirchner C, Kling R, Gruber Th and Waag A 2005 Appl. Phys. Lett. **87** 112104
[27] Gacic M, Jakob G, Herbort C, Adrian H, Tietze T, Brück S and Goering E 2007 Phys. Rev. B **75** 205206
[28] Ghoshal S and Anil Kumar P S 2008 J. Phys.: Cond. Matt. **20** 192201
[29] Khalid M and Esquinazi P 2012 Phys. Rev. B **85** 134424
[30] Sondheimer E H and Wilson A H 1947 Proc. Roy. Soc. (London) **A190** 435
[31] Khosla R P and Fischer J R 1970 Phys. Rev. B **2** 4084
[32] Appelbaum J A 1967 Phys. Rev. **154** 633
[33] Bridoux G, Villafuerte M, Ferreyra J M, Guimpel J, Nieva G, Figueroa C A, Straube B and Heluani S P 2018 Appl. Phys. Lett. **112** 092101
[34] Kuroyanagi A 1989 J. Appl. Phys. **66** 5492
[35] Patterson A 1939 Phys. Rev. **56** 978
[36] Nagaosa N, Sinova J, Onoda S, MacDonald A H and Ong N P 2010 Rev. Mod. Phys. **82** 1539
[37] Ziman J M 1960 *Electrons and Phonons: The Theory of Transport Phenomena in Solids* (Oxford: Clarendon Press)
[38] Shen L Y L and Rowell J M 1968 Phys. Rev. **165** 566
[39] Losee D L and Wolf E L 1969 Phys. Rev. **187** 925
[40] Alfaramawi K 2014 Bull. Mater. Sci. **37** 1603
[41] Arora N D, Hauser J R and Roulston D J 1982 IEEE Trans. Electron. Dev. **29** 292
[42] Debye P P and Conwell E M 1954 Phys. Rev. **93** 693
[43] Andrearczyk T, Jaroszyński J, Grabecki G, Dietl T, Fukumura T and Kawasaki M 2005 Phys. Rev. B **72** 121309R
[44] Mott N F 1973 *Electronics and Structural Properties of Amorphous Semiconductors* (London: Academic)
[45] Lee P A and Ramakrishnan T V 1985 Rev. Mod. Phys. **57** 287
[46] Ajimsha R S, Das A K, Misra P and Singh B 2017 J. Alloys and Compounds **708** 73-78
[47] Kawabata A 1980 J. Phys. Soc. Jpn. **49** 628